ELSEVIER

Biophysical Chemistry 134 (2008) 93 – 100

Biophysical Chemistry

http://www.elsevier.com/locate/biophyschem

Mad2 binding is not sufficient for complete Cdc20 sequestering in mitotic transition control (an *in silico* study)

Bashar Ibrahim [a,b], Peter Dittrich [a,b], Stephan Diekmann [c], Eberhard Schmitt [c,*]

[a] *Bio Systems Analysis Group, Institute of Computer Science, Friedrich-Schiller–University Jena, Ernst-Abbe-Platz 1-4, D-07743 Jena, Germany*
[b] *Jena Centre for Bioinformatics (JCB), Jena, Germany*
[c] *Biocomputing, Leibniz Institute for Age Research - FLI, Beutenbergstrasse 11, D-07745 Jena, Germany*

Received 30 September 2007; received in revised form 22 January 2008; accepted 22 January 2008
Available online 6 February 2008

Abstract

For successful mitosis, metaphase has to be arrested until all centromeres are properly attached. The onset of anaphase, which is initiated by activating the APC, is controlled by the spindle assembly checkpoint ^{M}SAC. Mad2, which is a constitutive member of the ^{M}SAC, is supposed to inhibit the activity of the APC by sequestering away its co-activator Cdc20. Mad1 recruits Mad2 to unattached kinetochores and is compulsory for the establishment of the Mad2 and Cdc20 complexes. Recently, based on results from *in vivo* and *in vitro* studies, two biochemical models were proposed: the Template and the Exchange model. Here, we derive a mathematical description to compare the dynamical behaviour of the two models. Our simulation analysis supports the Template model. Using experimentally determined values for the model parameters, the Cdc20 concentration is reduced down to only about half. Thus, although the Template model displays good metaphase-to-anaphase switching behaviour, it is not able to completely describe ^{M}SAC regulation. This situation is neither improved by amplification nor by p31^{comet} inhibition. We speculate that either additional reaction partners are required for total inhibition of Cdc20 or an extended mechanism has to be introduced for ^{M}SAC regulation.

Keywords: Mitotic control; Cdc20 sequestering; p31^{comet} inhibition; Kinetochore modeling; Template model; Exchange model

1. Introduction

Successful mitosis requires accurate chromosome segregation [1]. In eukaryotic cells, a cellular surveillance mechanism, the ^{M}SAC, suspends premature anaphase onset until all chromosomes are properly attached and have aligned on the mitotic spindle to guard the fidelity of chromosome segregation. Malfunction of the ^{M}SAC can generate aneuploidy [2,3] and contributes to cancer [4,5].

Anaphase is initiated by formation of the APC:Cdc20 complex [6], starting a cascade of enzymatic reactions [7,8], in the end cutting the cohesin rings [9]. The APC:Cdc20 complex cannot form during metaphase, because the APC (Anaphase Promoting Complex) is bound to the MCC (Mitotic Checkpoint Complex), and, in addition, Cdc20 (cell division cycle 20 homologue) concentration is low [1,10]. The latter is achieved by binding Cdc20 to Mad2, which is facilitated by Mad1, a positive regulator of the spindle checkpoint [10] (Mad: Mitotic arrest deficient). As the APC:Cdc20 complex is only allowed to form after the last kinetochore has attached, it is a fundamental question for a proper ^{M}SAC description, how APC:Cdc20 formation is suppressed until this moment.

Cdc20 appears in two forms, as free Cdc20 and bound to Mad2 [11]. APC is present as free APC and as part of the APC:MCC complex. As no inhibition mechanism is known to prevent APC:Cdc20 formation from free Cdc20 and free APC, both components cannot exist during metaphase at the same time. It is a generally accepted hypothesis that free Cdc20 is completely sequestered away, and for that reason the APC:Cdc20 complex is assumed to be unable to form.

* Corresponding author. Tel.: +49 3641 656269; fax: +49 3641 656210.
E-mail addresses: ibrahim@minet.uni-jena.de (B. Ibrahim), dittrich@minet.uni-jena.de (P. Dittrich), diekmann@fli-leibniz.de (S. Diekmann), eschmitt@fli-leibniz.de (E. Schmitt).

0301-4622/$ - see front matter © 2008 Elsevier B.V. All rights reserved.
doi:10.1016/j.bpc.2008.01.007

Table 1
Initial concentrations for all species at start of simulation run (values taken from literature)

Species	Initial concentration	Reference
[Cdc20]	2.2×10^{-7} M	[30,16,34]
[Mad1]	0.5×10^{-7} M	[30,16,34]
[O-Mad2]	1.5×10^{-7} M	[30,16,34]
[C-Mad2]	0.1875×10^{-7} M	[30,16,34]
[Mad1:C-Mad2]	0.5×10^{-7} M	[30,16,34]
[$p31^{comet}$]	10.0×10^{-7} M	[17,28]

All other initial concentrations are 0.

The formation of the Cdc20:Mad2 complex has been recently described biochemically, leading to two different models: The "Exchange" model [11] and the "Template" model [12]. In the Exchange model it is assumed that Mad1 recruits open Mad2 (O-Mad2) at the kinetochore and transforms its conformation from O-Mad2 to closed Mad2 (C-Mad2). C-Mad2 then dissociates from Mad1 and binds Cdc20. This model portrays Mad1 as a catalyst of the structural transition of O-Mad2 into C-Mad2. Already this purely biochemical description gave rise to several criticisms [13,14]. Especially the question remained, why and how Mad2 first binds (as O-Mad2) to Mad1, but then dissociates off (as C-Mad2) [15]. In a subsequent sophisticated experimental investigation, [12] could precise the reaction mechanism further and developed a second model, the biochemical Template model. Here, it is assumed that Mad1 and C-Mad2 form a stable core complex at unattached kinetochores. This core then binds additional molecules of O-Mad2 through formation of conformational heterodimers between the C-Mad2 subunit of the Mad1:C-Mad2 complex and O-Mad2. Cdc20 binding to this complex leads to the conversion of O-Mad2 to C-Mad2 resulting in the formation of Cdc20:C-Mad2, which in turn is assumed then to dissociate off Mad1:C-Mad2 [16]. But even with this refined description, many questions remained open [17,18], and a decision for one of the models to be more realistic could not be met [19].

To address the question, how Cdc20 concentration relates to anaphase onset and how it is regulated, we investigated the role of Mad1 in eliciting the formation of the Cdc20:Mad2 complex on the basis of these two biochemical models. To this end, we derived the reaction equations from the description in [11,12]. Using standard principles of chemistry and thermodynamics, we converted the reaction equations into non-linear ordinary differential equations for the concentrations of the reactants. To simulate their dynamics in the course of time, the differential equations were integrated for different values of the kinetic constants involved. To find a behaviour in concordance with experimental results, we employed a minimization procedure.

The purpose of this paper is threefold. First, we show how to derive a mathematical model for the biochemically described Exchange and Template models. Then, as the main purpose, we compare the two models by mathematical simulations and show that the Exchange model is not able to realistically describe the metaphase-to-anaphase transition. Though the Template model in principle can show correct switching behaviour for this transition, it is not able to sequester away Cdc20 completely whenever physiologically realistic kinetic constants are used. Therefore, in a third step, we investigate six further extensions of the Template model, based on recently described biochemical amplification and inhibition effects, especially considering the role of $p31^{comet}$. As total inhibition of Cdc20 activity during metaphase is the basis of most models for metaphase-to-anaphase transition [20–22], it is an important question, whether additional reaction partners are required for total Cdc20 inhibition or an extended ^{M}SAC regulation mechanism has to be introduced.

2. Methods: definition and simulation of the models

For each model, we describe briefly the basic biochemical pathways and experimental findings. These experimental foundations are turned into chemical reaction equations. In some cases, reactions depend on the attachment of the microtubules to the kinetochore, which is described by a switching parameter u: before attachment, we set $u=1$; and after attachment, $u=0$. Formation of the Mad1:C-Mad2:O-Mad2* complex in the classical Template model is an example for this dependence (see Eq. (6)). The corresponding kinetic parameter α_T is therefore multiplied by u. Biochemically, the switching parameter u may represent the function of dynein, which after microtubule attachment removes the Mad1:C-Mad2 2:2 complex from the kinetochore site.

The reaction equations are converted into ordinary differential equations (ODEs) using the mass action kinetics (c.f. Supplement A–E). Starting from initial concentrations for all reaction partners taken from literature (cf. Table 1), the ODEs are integrated until steady state is reached before attachment (using $u=1$). After switching u to 0, the equations are again integrated, until steady state is reached. The minimum concentration of Cdc20 before attachment and the recovery after attachment (level of Cdc20 increase and recovery time) are criteria to compare the models.

As far as documented in the literature, experimental values are used for the kinetic constants. In all other cases, we select representative values for each parameter (cf. Tables 2 and 3) exemplifying its whole physiologically possible range. The resulting concentration curves show the influence of the kinetic parameter on the behaviour of the model. It can be clearly

Table 2
Kinetic parameters for the Template model and its variations

Parameter	Value	Reference
α_T	2×10^{5} M^{-1} s^{-1}	[19]
β_T	0.2 s^{-1}	[19]
δ_T	1.7×10^{6} M^{-1} s^{-1}	[19]
ζ_T	0.037 s^{-1}	[19]
k_4	10^{3}–10^{5} M^{-1} s^{-1}	This study
k_{-4}	0.03 s^{-1}	This study
k_5	10^{3}–10^{5} M^{-1} s^{-1}	This study
γ_T	10^{3}–10^{9} M^{-1} s^{-1}	This study
η_T	5×10^{-4}–10^{-1} s^{-1}	This study
ζ_T	10^{3}–10^{5} M^{-1} s^{-1}	This study
σ_T	0.03 s^{-1}	This study

The values not taken from literature are designated 'this study' and were varied within the range indicated.

Table 3
Kinetic parameters for the Exchange model

Parameter	Value	Reference
k_1	3×10^{-5} s^{-1}	[11]
k_{-1}	5.2×10^{-6} s^{-1}	[11]
α_E	4×10^{3} M^{-1} s^{-1}	[11]
k_{-2}	1.5×10^{-2} s^{-1}	[11]
k_3	2.8×10^{-4} s^{-1}	[11]
k_{-3}	23 M^{-1} s^{-1}	[11]
γ_E	10^{5}–10^{9} M^{-1} s^{-1}	This study
η_E	3×10^{-5}–10^{-2} s^{-1}	This study

The values not taken from literature are designated 'this study' and were varied within the range indicated.

seen that the variation of the curves depends in a continuous manner on the variation of the parameters. Their influence on the behaviour of the models is described in detail in the respective sections. In a more global approach, we fit optimal values to the model parameters by minimizing a Cdc20 concentration objective functional describing a minimal Cdc20 concentration before and a maximal concentration after switching (see Supplement F). Minimization was performed by statistical approaches by selecting randomly starting values within the whole range of parameters. For the Cdc20 concentration functional, a minimal solution is in general not unique, as can be seen from the graphs with the example parameter settings. On the other hand, due to the continuous behaviour of the system in dependence of the parameters, in some cases parameters tend to an asymptotic, often physiologically unrealistic, value. In other cases, the velocity of Cdc20 recovery after switching can help to define a possible parameter set. The details are explained in the respective model sections.

3. Biochemical basis of the models

The biochemical basis of the models are the binding kinetics of Mad1, Mad2, and Cdc20. Mad1 forms a tight 2:2 complex with Mad2 [23]. Binding of Mad2 to Mad1 triggers a conformational change of Mad2, in a similar way as does Cdc20 binding: Mad2 binds to Mad1 and Cdc20 in the same pocket with similar affinities [24]. Mad2 can adopt two conformations, O-Mad2 and C-Mad2, differing in the structure of its 50 residue C-terminal segment [24]. The O-Mad2 is the physiological state of cytosolic Mad2 in the absence of Mad1 or Cdc20 [11]. O-Mad2 refolds to C-Mad2 when bound to the kinetochore receptor Mad1 or the APC activator Cdc20 [11]. Upon microtubule attachment, Mad1 [25] remains detectable at kinetochores whereas Mad2 [26] depletes from the kinetochores.

3.1. The Mad2 "Exchange" model

In order to explain the formation of the Mad2:Cdc20 complex, Luo et al. [11] suggested the Mad2 Exchange model, based on a series of *in vitro* and *in vivo* experiments. It assumes that Mad1 recruits open Mad2 (O-Mad2) at the kinetochore and transforms its conformation from O-Mad2 to closed Mad2 (C-Mad2). C-Mad2 then dissociates away from Mad1 and binds Cdc20. This model portrays Mad1 as a catalyst of the structural transition of O-Mad2 into C-Mad2. The reaction rules governing the Exchange model are (cf. Fig. 1b):

$$\text{O-Mad2} \underset{k_{-1}}{\overset{k_1}{\rightleftharpoons}} \text{C-Mad2} \tag{1}$$

$$\text{Mad1} + \text{O-Mad2} \underset{k_{-2}}{\overset{\alpha_E.u}{\rightleftharpoons}} \text{Mad1:C-Mad2} \tag{2}$$

$$\text{Mad1:C-Mad2} \underset{k_{-3}}{\overset{k_3}{\rightleftharpoons}} \text{C-Mad2} + \text{Mad1} \tag{3}$$

$$\text{C-Mad2} + \text{Cdc20} \xrightarrow{\gamma_E} \text{Cdc20:C-Mad2} \tag{4}$$

$$\text{Cdc20:C-Mad2} \xrightarrow{\eta_E} \text{Cdc20} + \text{O-Mad2} \tag{5}$$

which lead to the set of time dependent non-linear ODEs listed in Supplement A, Eqs. (S13–S18).

The only parameter dependent on the kinetochore attachment status is α_E which therefore is multiplied by the switching parameter u. The reaction scheme contains the background reaction for O-Mad2 conversion to C-Mad2 (Eq. (1)) with very low rates k_1 and k_{-1} [11]. For α_E, k_{-2}, k_3, and k_{-3} we used quantitative experimental data from [11] (see Table 3). The remaining two parameters γ_E and η_E were varied within a realistic range [11,12,16]: γ_E between 10^5 M^{-1} s^{-1} and 10^9 M^{-1} s^{-1} and η_E between $3*10^{-5}$ s^{-1} and 10^{-2} s^{-1}. When analysing this set of ODEs, we found that only for very small η_E ($3*10^{-5}$ s^{-1}) the initial Cdc20 concentration is clearly reduced to about half the initial value (Fig. S5a) while for the higher values of η_E (10^{-2} s^{-1}) the Cdc20 concentration hardly changed (Fig. S5d). Our data indicate that the switching of u from 1 to 0 has little influence on Cdc20 concentration, smaller η_E (Fig. S5a) showing slightly larger effects than larger η_E (Fig. S5d). A large influence of u on Cdc20 concentration, however, is required for checkpoint function. While the ^{M}SAC is activated, the concentration of Cdc20 should be low, and should switch to large values when the kinetochores are attached. The Exchange model does not describe this behaviour.

3.2. The "Template" model

In the Exchange model it remained unclear, how Mad2 first binds to Mad1 and then dissociates off by just adopting another conformation. In an experimental study, [12] provided information about the detailed reaction mechanism, which was finally condensed into the Mad2 Template model. It assumes that Mad1 and C-Mad2 form a stable core complex at unattached kinetochores [12]. This core then binds additional molecules of O-Mad2 through formation of conformational heterodimers between the C-Mad2 subunit of the Mad1:C-Mad2 complex and O-Mad2. Cdc20 binding to this complex leads to the conversion of O-Mad2 to C-Mad2 resulting in the formation of Cdc20:C-Mad2, which in turn is assumed then to dissociate off Mad1:C-Mad2 [16]. Upon Mad1:C-Mad2 binding, O-Mad2 adopts an

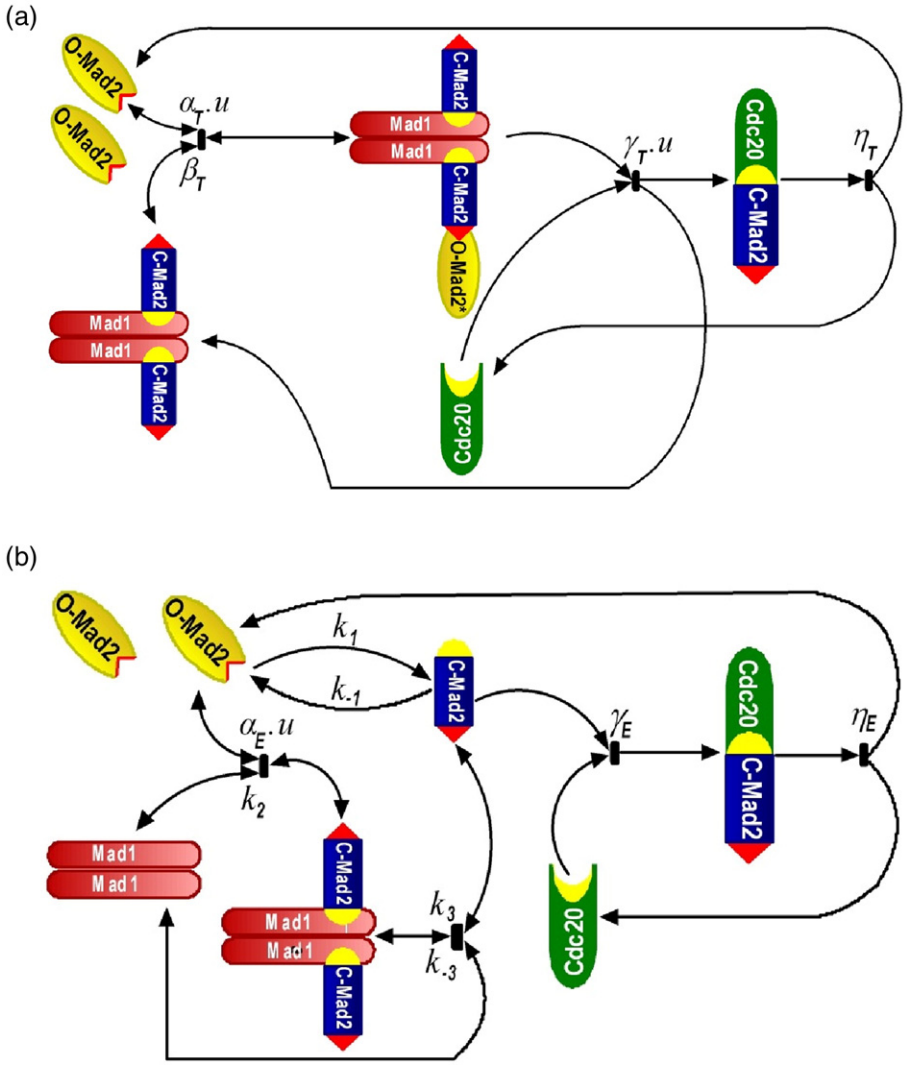

Fig. 1. Schematic reaction networks of the Template model (a) and the Exchange model (b).

intermediate conformation (O-Mad2*) that can quickly and efficiently bind Cdc20 and switch to the C-conformation (see Fig. 1a). The reaction rules covering the Template model are (cf. Supplement B for ODEs):

$$\text{Mad1:C-Mad2} + \text{O-Mad2} \underset{\beta_T}{\overset{\alpha_T.u}{\rightleftharpoons}} \text{Mad1:C-Mad2:O-Mad2*} \quad (6)$$

$$\text{Mad1:C-Mad2:O-Mad2*} + \text{Cdc20} \xrightarrow{\gamma_T.u} \text{Cdc20 :C-Mad2} + \text{Mad1:C-Mad2} \quad (7)$$

$$\text{Cdc20:C-Mad2} \xrightarrow{\eta_T} \text{Cdc20} + \text{O-Mad2} \quad (8)$$

The kinetic constants α_T, β_T, and γ_T depend on the attachment state of the kinetochore and are thus multiplied by the variable u. We used quantitative data from FRAP experiments for α_T and β_T [19]. The remaining two parameters γ_T and η_T were varied widely within realistic frames [11,12,16]: η_T between $5*10^{-4}$ s^{-1} and 10^{-1} s^{-1}, and γ_T between 10^5 M^{-1} s^{-1} and 10^9 M^{-1} s^{-1} (c.f. Table 2). Characteristic Cdc20 concentration curves were obtained as displayed in Figs. 2 and S4.

For η_T values smaller than 10^{-1} s^{-1}, we observed a clear dependence of the Cdc20 concentration on the switching parameter u with the effect being larger for larger γ_T. In early mitosis ($u=1$), for η_T values in the order of 10^{-3} s^{-1} (clearly smaller than 10^{-2} s^{-1}) and γ_T values larger than 10^6 M^{-1} s^{-1}, the Template model sequesters about half of the Cdc20 concentration (Fig. 2) in quantitative agreement with experimental findings [11,16]. However, within this frame of realistic parameter variations, Cdc20 is never completely inhibited as would be required for checkpoint function. η_T determines the rate of Cdc20 concentration recovery after u is switched to zero: small η_T values of about 10^{-3} s^{-1} display slow recovery while values of 10^{-2} s^{-1} and above show fast recovery (Figs. 2 and S4).

Already Fang [16] increased the Mad2 level 100fold (to 22.5 μM) to gain maximal Cdc20 inhibition. In our Template model simulation, an 8fold increase of free Mad2 concentration showed complete Cdc20 disappearance for small η_T

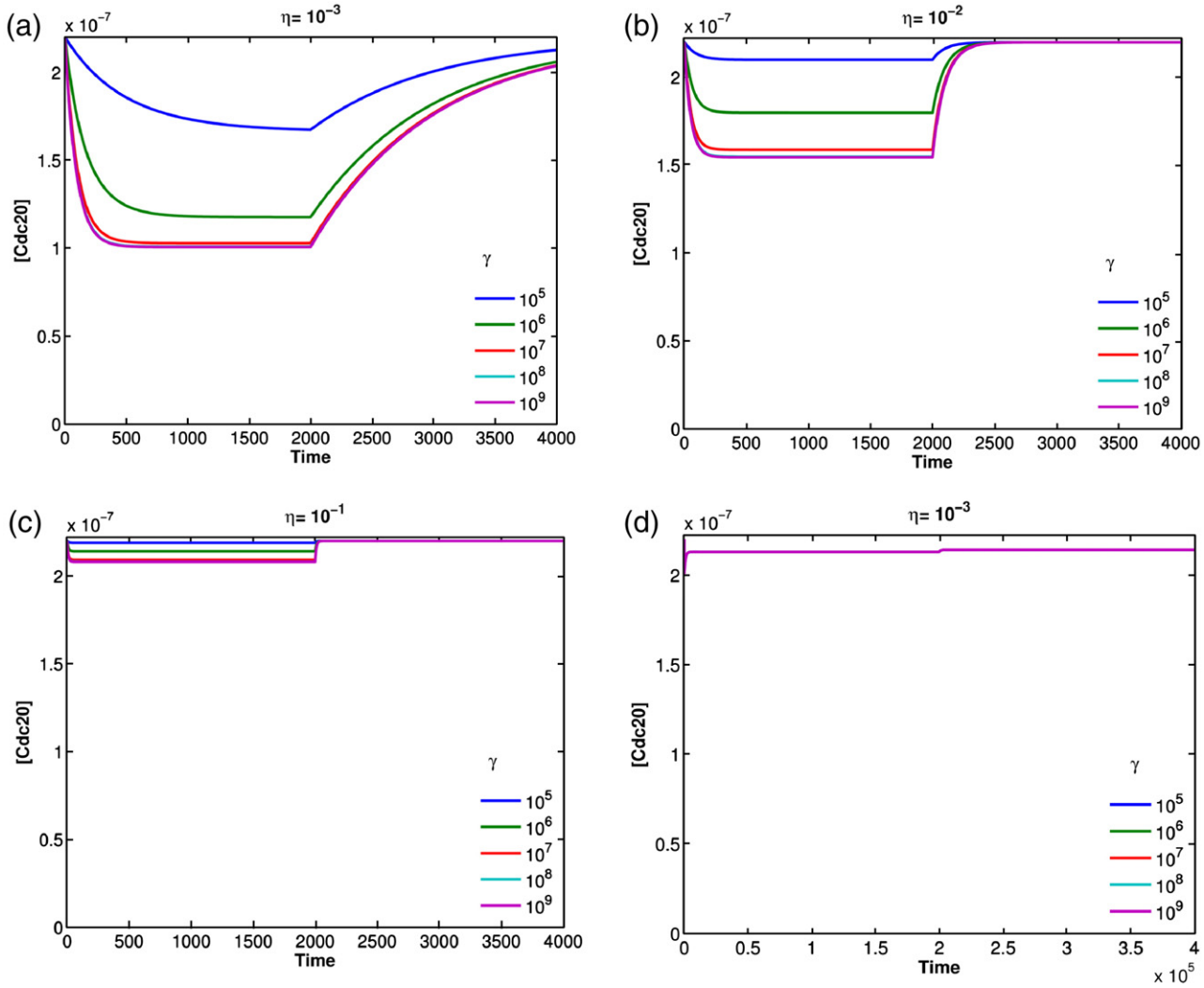

Fig. 2. The dynamical behaviour of the Template model (a–c) with different values of γ and η_T (time in s). Only η_T-values between 10^{-3} and 10^{-2} show acceptable switching behaviour. For comparison, the dynamical behaviour of the Exchange model ((d) for $\eta_E = 10^{-3}$) does not show any switching for $10^{-4} < \eta_E < 0.1$.

($\leq 10^{-2}$ s^{-1}) and large γ_T ($>10^6$ M^{-1} s^{-1}) (see Fig. S4). In addition, the rate of Cdc20 recovery becomes fast for larger values of η_T. However, this Mad2 concentration is far above experimentally observed values [16].

3.3. Variations of the Template model

In the Template model, for realistic parameter ranges, Cdc20 inhibition is not as high as anticipated. We therefore modified the model according to recent experimental results.

3.3.1. Amplification effects

DeAntoni et al. [12] hypothesized that in analogy to the reactions in Eqs. (6) and (7) based on Mad1, Cdc20:C-Mad2 can also be formed by the reactions in Eqs. (9) and (10) below based on Cdc20. This additional pathway for the production of Cdc20:C-Mad2 results in a signal amplification for the ^{M}SAC since Cdc20:C-Mad2 now is produced not only at the location of Mad1 at the kinetochore but at a larger number of locations everywhere in the cell. To check the effect of this additional pathway, we added two reactions (9–10) to the Template model (see Fig. S3a, ODEs Supplement C):

$$\text{Cdc20:C-Mad2} + \text{O-Mad2} \underset{k_{-4}}{\overset{k_4}{\rightleftharpoons}} \text{Cdc20:C-Mad2:O-Mad2*} \tag{9}$$

$$\text{Cdc20:C-Mad2:O-Mad2*} + \text{Cdc20} \xrightarrow{k_5} 2\text{Cdc20:C-Mad2} \tag{10}$$

The Mad2 heterodimer formation at the Mad1 location is considered to be as fast as at Cdc20, so that k_4 and k_5 would be as large as α_T and γ_T, respectively. For k_4 and k_5 both equal to 10^5 M^{-1} s^{-1}, $\eta_T = 10^{-3}$ s^{-1} and γ_T in the range between 10^5 M^{-1} s^{-1} and 10^9 M^{-1} s^{-1}, our calculations indicate that the switching parameter u has little to no effect on the Cdc20 concentration (Fig. S6b). Small $k_4 = k_5 = 10^3$ M^{-1} s^{-1} have vanishing influence on the model and roughly show the Template model behaviour as observed before (Fig. S6a). Furthermore, using our fitting procedure for optimal parameters,

the values of k_4 and k_5 tend to zero: the amplification is discarded from the reaction scheme.

The additional amplification reactions could contribute to the model behaviour, in case the reaction Eq. (9) did not take place all the time, but instead would also be controlled by the switching parameter u (k_4 replaced by $k_4.u$). With the same parameter values as in the previous calculation (Fig. S6d), we obtained Cdc20 concentrations nearly independent from γ_T: low Cdc20 concentrations were reached now also for small values of γ_T (Fig. S6c). However, we have no experimental indication for such an influence of microtubule attachment to kinetochores on k_4.

3.3.2. Inhibition effects

Another way to vary the Template model is the introduction of the Mad2 ligand p31^{comet} (formerly CMT2), which is a negative regulator of the spindle checkpoint. It prevents further Mad2 turnover on Mad1 and neutralizes the inhibitory activity of Cdc20-bound Mad2, leading to activation of APC followed by degradation of Securin and Cyclin B [27]. Its negative effect on the ^{M}SAC is based on its competition with O-Mad2 for C-Mad2 binding [27,28]. It forms triple complexes with C-Mad2 and either Mad1 or Cdc20 [28]. If p31^{comet} is activated at microtubule attachment to the kinetochores, it might be a cellular factor contributing to the checkpoint switching behaviour. Therefore, we introduced an additional reaction (11) into the Template model reactions (6–8) describing the effect of p31^{comet} (ODEs Supplement D):

$$\text{Mad1:C-Mad2} + \text{p31} \underset{\zeta_T}{\overset{\delta_T.v}{\rightleftharpoons}} \text{Mad1:C-Mad2:p31} \qquad (11)$$

The activation of p31^{comet} is taken care of by the introduction of the switching parameter v which is equal to zero until the kinetochores are attached and switches to one afterwards. In fact, the function of the switching parameter u can be totally replaced by p31^{comet} inhibition, as the p31^{comet} system with $u=1$ all the time shows the same dynamic results as the unmodified Template model (Fig. 2). Combining both effects (u and v switching) still show the same dynamics.

3.3.3. Amplification plus inhibition effects

Including both, amplification and p31^{comet} inhibition, into the Template model, we obtain the chemical reaction scheme (see Fig. S3b), consisting of Eqs. (6–8), (9–11), and an additional Eq. (12), (ODEs Supplement E):

$$\text{Cdc20:C-Mad2} + \text{p31} \underset{\sigma_T}{\overset{\xi_T.v}{\rightleftharpoons}} \text{Cdc20:C-Mad2:p31} \qquad (12)$$

For $u=1$ before and after attachment (all the time), the model behaviour is not influenced before switching ($v=0$). After switching ($v=1$), for low $\xi_T=10^3$ M^{-1} s^{-1}, the new additional reaction mechanism is slightly less effective in Cdc20 recovery, whereas for high $\xi_T=10^5$ M^{-1} s^{-1}, Cdc20 cannot recover since it is incorporated into the triple complex with C-Mad2 and p31^{comet}. Combining u and v switching does not change the dynamics.

4. Discussion

The mitotic checkpoint proteins Mad1, Mad2 and Cdc20 play an essential role in cell cycle control by contributing to the regulation of the ^{M}SAC mechanism [12]. Their interactions have been studied experimentally (e.g. [11,12,16]) resulting in two alternative models describing their behaviour, the “Exchange” [11] and the “Template model” [12]. Recently, experimental data questioned the validity of the Exchange model while they supported the Template model [17–19]. Here, the two models were described by sets of chemical reactions, which were transformed into sets of non-linear ordinary differential equations (ODEs). The ODEs quantitatively display the dynamic behaviour of the models. Where experimental results were available, parameters were chosen according to these data. The unknown systems parameters were optimized according to the known behaviour of the Cdc20 concentration at the metaphase to anaphase transition (Supplement F).

The Exchange model was suggested by Luo et al. [11] in order to explain their experimental data. This model, however, had been criticized because it is unable to explain additional experimental data from other groups [1,17–19] and since it assumes that Mad1 competes with Cdc20 for Mad2 binding. We identified an additional weakness of the Exchange model: it is hardly able to show switching kinetics. This property is model inherent since those reactions involving Cdc20 are kinetochore uncontrolled and are not influenced by microtubule attachment. Moreover, the steady state is reached very slowly (about 100 times slower than in the Template model). In addition, when applying experimentally determined parameter values, the Exchange model is not able to sequester Cdc20 sufficiently as would be required for ^{M}SAC regulation. Even a free parameter optimization did not result in a satisfying model switching behaviour.

In contrast, the behaviour of the Mad2 Template model [12] is in accordance with experimental observations [16,17,19] and shows robust switching behaviour. However, the Cdc20 concentration is only reduced down to about half when experimentally determined values are used for the model parameters. This observation is in agreement with Fang [16], and Luo et al. [11] in HeLa cells. Complete sequestering of Cdc20 is obtained for higher Mad2 concentrations, as observed by Fang (for a 100fold higher Mad2 concentration). When increasing the free Mad2 concentration 8fold in the Template model, we found complete reduction of Cdc20 concentration. However, there is no experimental indication for such a high Mad2 concentration in HeLa cells. Thus, although showing robust switching behaviour when using experimentally determined parameter values, the Template model as listed is unable to result in complete inhibition of Cdc20. This conclusion is in agreement with statements of Fang [16]. Contributions from additional reaction partners are required for complete Cdc20 sequestering. Such a reaction partner seems to be the checkpoint protein BubR1 which also binds Cdc20 [16,29,30] and cooperates to form the mitotic checkpoint complex MCC [29].

Mad2 heterodimers can bind to either Mad1 or Cdc20 [12,15]. Thus, C-Mad2:Cdc20 complexes can be formed not

only at Mad1 kinetochore sites but in the whole cell, amplifying complex formation. To investigate the amplification mechanism, we extended the Template model by the appropriate reactions. When the newly introduced reaction rates are small, these reactions do not contribute to the model behaviour. If however the rates are high, there is hardly any Cdc20 recovery after switching since these amplification reactions are not influenced by mitotic progression. Thus, these additional reactions do not improve Template model behaviour.

The checkpoint inhibitor $p31^{comet}$ competes with O-Mad2 for C-Mad2 binding, thus preventing the binding of O-Mad2 to C-Mad2 [17,27,31]. It binds to the surface of C-Mad2 opposite to Mad1 and Cdc20 [17,19], forming triple complexes with these proteins. If $p31^{comet}$ is activated at metaphase to anaphase transition, our model calculations clearly show that $p31^{comet}$ is able to introduce switching behaviour into the model and would be even able to replace the function of the switching parameter u: The Template model behaviour is very similar when u is removed and $p31^{comet}$ reactions are added to the model. The situation is slightly different in the presence of the amplification reactions. Now, removing u and introducing the $p31^{comet}$ reactions, we found no improved Cdc20 recovery for small reactions rates ξ_T, however, strongly reduced recovery for large ξ_T rates. In order to distinguish between these two cases, additional experimental kinetic data are required for $p31^{comet}$ reactions. In general we observe that $p31^{comet}$ is not sufficient for full ^{M}SAC regulation. This finding is particularly interesting, because it was shown in a very general model that amplification reactions might be necessary to promote the final signal from the last attaching kinetochore for anaphase onset [32,33]. In [32], $p31^{comet}$ is explicitly mentioned as a candidate for this information transmission.

The switching parameter u represents the function of dynein which after microtubule attachment removes the Mad1:C-Mad2 2:2 complex from the kinetochore site. It might also represent potential additional functions which contribute to switching behaviour. When both, u and $p31^{comet}$, are included in the reaction scheme, the general behaviour of the system is not improved over those systems including only u or only $p31^{comet}$. We observed an improvement however, when the reaction Eq. (9) becomes controlled by u. Now, before attachment, low concentrations for Cdc20 were observed even for low values of γ_T, and after attachment Cdc20 recovers fast independent of γ_T values, showing an considerably improved regulation behaviour. However, we have no experimental indication for a mitotic control of reaction Eq. (9).

Taken together we conclude, that the presented Exchange model is not describing checkpoint function. The Template model is clearly superior and shows robust switching behaviour. However, applying experimentally determined parameter values to this model, Cdc20 is not sequestered completely. Additional reaction partners would be required for total inhibition of free Cdc20. BubR1 would be a potential candidate for this function. Thus, as a next step, MCC formation including BubR1 and Cdc20 will be included into the quantitative analysis. In addition, biochemical experiments are carried out presently in our lab to reveal the location and time resolved dynamics of protein binding to the kinetochore.

Acknowledgements

We would like to thank the German Academic Exchange Service (DAAD, grant A/04/31166) and the Federal Ministry of Education and Research (BMBF, grant 0312704A) for the financial support. We acknowledge the optimizer [35] validation by Thorsten Lenser. We also thank the unknown reviewers for encouraging us to extend the manuscript.

Appendix A. Supplementary data

Supplementary data associated with this article can be found, in the online version, at doi:10.1016/j.bpc.2008.01.007.

References

[1] A. Musacchio, E.D. Salmon, The spindle-assembly checkpoint in space and time, Nat. Rev. Mol. Cell Biol. 8 (2007) 379–393.
[2] M. Kim, G.D. Kao, Newly identified roles for an old guardian: profound deficiency of the mitotic spindle checkpoint protein BubR1 leads to early aging and infertility, Cancer Biol. Ther. 4 (2005) 164–165.
[3] N. Steuerwald, Meiotic spindle checkpoints for assessment of aneuploid oocytes, Cytogenet. Genome Res. 111 (2005) 256–259.
[4] D.A. Compton, Chromosomes walk the line, Nat. Cell Biol. 8 (2006) 308–310.
[5] A. Gupta, S. Inaba, O.K. Wong, G. Fang, J. Liu, Breast cancer-specific gene 1 interacts with the mitotic checkpoint kinase BubR1, Oncogene 22 (2003) 7593–7599.
[6] H. Yu, Regulation of APC-Cdc20 by the spindle checkpoint, Curr. Opin. Cell Biol. 14 (2002) 706–714.
[7] J.-M. Peters, The anaphase-promoting complex: proteolysis in mitosis and beyond, Mol. Cell 9 (2002) 931–943.
[8] K.M. May, K.G. Hardwick, The spindle checkpoint, J. Cell Sci. 119 (2006) 4139–4142.
[9] H. Yu, Z. Tang, Bub1 multitasking in mitosis, Cell Cycle 4 (2005) 262–265.
[10] R.H. Chen, D.M. Brady, D. Smith, A.W. Murray, K.G. Hardwick, The spindle checkpoint of budding yeast depends on a tight complex between the Mad1 and Mad2 proteins, Mol. Biol. Cell 10 (1999) 2607–2618.
[11] X. Luo, Z. Tang, G. Xia, K. Wassmann, T. Matsumoto, J. Rizo, H. Yu, The Mad2 spindle checkpoint protein has two distinct natively folded states, Nat. Struct. Mol. Biol. 11 (2004) 338–345.
[12] A. DeAntoni, C.G. Pearson, D. Cimini, J.C. Canman, V. Sala, L. Nezi, M. Mapelli, L. Sironi, M. Faretta, E.D. Salmon, A. Musacchio, The Mad1/Mad2 complex as a template for Mad2 activation in the spindle assembly checkpoint, Curr. Biol. 15 (2005) 214–225.
[13] P. Lenart, J.-M. Peters, Checkpoint activation: do not get mad too much, Curr. Biol. 16 (2006) R412–R414.
[14] K.G. Hardwick, Checkpoint signalling: Mad2 conformers and signal propagation, Curr. Biol. 15 (2005) R122–R124.
[15] A. DeAntoni, V. Sala, A. Musacchio, Explaining the oligomerization properties of the spindle assembly checkpoint protein Mad2, Philos. Trans. R. Soc. Lond., B Biol. Sci. 360 (2005) 637–648.
[16] G. Fang, Checkpoint protein BubR1 acts synergistically with Mad2 to inhibit anaphase-promoting complex, Mol. Biol. Cell 13 (2002) 755–766.
[17] M. Mapelli, F.V. Filipp, G. Rancati, L. Massimiliano, L. Nezi, G. Stier, R.S. Hagan, S. Confalonieri, S. Piatti, M. Sattler, A. Musacchio, Determinants of conformational dimerization of Mad2 and its inhibition by p31comet, EMBO J. 25 (2006) 1273–1284.
[18] L. Nezi, G. Rancati, A. DeAntoni, S. Pasqualato, S. Piatti, A. Musacchio, Accumulation of Mad2-Cdc20 complex during spindle checkpoint activation requires binding of open and closed conformers of Mad2 in *Saccharomyces cerevisiae*, J. Cell Biol. 174 (2006) 39–51.
[19] M. Vink, M. Simonetta, P. Transidico, K. Ferrari, M. Mapelli, A.D. Antoni, L. Massimiliano, A. Ciliberto, M. Faretta, E.D. Salmon, A. Musacchio, In

vitro FRAP identifies the minimal requirements for Mad2 kinetochore dynamics, Curr. Biol. 16 (2006) 755–766.
[20] B. Ibrahim, P. Dittrich, S. Diekmann, E. Schmitt, Stochastic effects in a compartmental model for mitotic checkpoint regulation, J. Integr. Bioinformatics 4 (3) (2007) 66 Online Journal: http://journal.imbio.de/index.php?paper_id=66.
[21] A. Toth, E. Queralt, F. Uhlmann, B. Novak, Mitotic exit in two dimensions, J. Theor. Biol. 248 (2007) 560–573.
[22] E. Queralt, C. Lehane, B. Novak, F. Uhlmann, Downregulation of PP2A (Cdc55) phosphatase by separase initiates mitotic exit in budding yeast, Cell 125 (2006) 719–732.
[23] L. Sironi, M. Melixetian, M. Faretta, E. Prosperini, K. Helin, A. Musacchio, Mad2 binding to Mad1 and Cdc20, rather than oligomerization, is required for the spindle checkpoint, EMBO J. 20 (2001) 6371–6382.
[24] X. Luo, Z. Tang, J. Rizo, H. Yu, The Mad2 spindle checkpoint protein undergoes similar major conformational changes upon binding to either Mad1 or Cdc20, Mol. Cell 9 (2002) 59–71.
[25] M.S. Campbell, G.K. Chan, T.J. Yen, Mitotic checkpoint proteins HsMAD1 and HsMAD2 are associated with nuclear pore complexes in interphase, J. Cell Sci. 114 (2001) 953–963.
[26] M.A. Lampson, T.M. Kapoor, The human mitotic checkpoint protein BubR1 regulates chromosome-spindle attachments, Nat. Cell Biol. 7 (2005) 93–98.
[27] T. Habu, S.H. Kim, J. Weinstein, T. Matsumoto, Identification of a MAD2-binding protein, CMT2, and its role in mitosis, EMBO J. 21 (2002) 6419–6428.
[28] G. Xia, X. Luo, T. Habu, J. Rizo, T. Matsumoto, H. Yu, Conformation-specific binding of p31(comet) antagonizes the function of Mad2 in the spindle checkpoint, EMBO J. 23 (2004) 3133–3143.
[29] V. Sudakin, G.K. Chan, T.J. Yen, Checkpoint inhibition of the APC/C in heLa cells is mediated by a complex of BubR1, Bub3, Cdc20, and Mad2, J. Cell Biol. 154 (2001) 925–936.
[30] Z. Tang, R. Bharadwaj, B. Li, H. Yu, Mad2-Independent inhibition of APCCdc20 by the mitotic checkpoint protein BubR1, Dev. Cell 1 (2001) 227–237.
[31] H. Yu, Structural activation of Mad2 in the mitotic spindle checkpoint: the two-state Mad2 model versus the Mad2 Template model, J. Cell Biol. 173 (2006) 153–157.
[32] A. Doncic, E. Ben-Jacob, N. Barkai, Evaluating putative mechanisms of the mitotic spindle checkpoint, Proc. Natl. Acad. Sci. U. S. A. 102 (2005) 6332–6337.
[33] R.P. Sear, M. Howard, Modeling dual pathways for the metazoan spindle assembly checkpoint, Proc. Natl. Acad. Sci. U. S. A. 103 (2006) 16758–16763.
[34] B.J. Howell, D.B. Hoffman, G. Fang, A.W. Murray, E.D. Salmon, Visualization of Mad2 dynamics at kinetochores, along spindle fibers, and at spindle poles in living cells, J. Cell Biol. 150 (2000) 1233–1250.
[35] N. Hansen, S.D. Muller, P. Koumoutsakos, Reducing the time complexity of the derandomized evolution strategy with covariance matrix adaptation (CMA-ES), Evol. Comput. 11 (2003) 1–18.